A Novel Protein Involved in the Functional Assembly of the Oxygen-Evolving Complex of Photosystem II in *Synechocystis* sp. PCC 6803†

Galyna I. Kufryk* and Wim F. J. Vermaas

Department of Plant Biology and Center for the Study of Early Events in Photosynthesis, Arizona State University, Box 871601, Tempe, Arizona 85287-1601

Received November 17, 2000; Revised Manuscript Received May 23, 2001

ABSTRACT: Mutation of Glu69 to Gln in the D2 protein of photosystem II is known to lead to a loss of photoautotrophic growth in *Synechocystis* sp. PCC 6803. However, second-site mutants (pseudorevertants) with restored photoautotrophic growth but still maintaining the E69Q mutation in D2 are easily obtained. Using a genomic mapping technique involving functional complementation, the secondary mutation was mapped to *slr0286* in two independent mutants. The mutations in Slr0286 were R42M or R394H. To study the function of Slr0286, mutants of E69Q and of the wild-type strain were made that lacked *slr0286*. Deletion of *slr0286* did not affect photoautotrophic capacity in wild type but led to a marked decrease in the apparent affinity of Ca^{2+} to its binding site at the water-splitting system of photosystem II and to a reduced heat tolerance of the oxygen-evolving system, particularly in E69Q. Moreover, a small increase in the half-time for photoactivation of the oxygen-evolving complex of photosystem II for both wild type and the E69Q mutant was observed in the absence of Slr0286. The accumulation of photosystem II reaction centers, dark stability of the oxygen-evolving apparatus, stability of oxygen evolution, and the kinetics of charge recombination between Q_A^- and the donor side were not affected by deletion of *slr0286*. Slr0286 lacks clear functional motifs, and no homologues are apparent in other organisms, even not in other cyanobacteria. In any case, Slr0286 appears to help the functional assembly and stability of the water-splitting system of photosystem II.

Photosystem II (PS II)[1] (*1*−*3*) is one of the major components of the photosynthetic apparatus of cyanobacteria and higher plants. This photosystem catalyzes light-driven electron transport from water to the plastoquinone pool in thylakoid membranes, resulting in formation of molecular oxygen. Most components of PS II are similar in cyanobacteria and higher plants (*4*, *5*). The water-splitting complex of PS II consists of a cluster of Mn ions liganded by one or more polypeptides. The D1 protein is central to the oxygen-evolving cluster (*6*−*8*), but the D2 (*9*), CP43 (*10*), and CP47 (*11*, *12*) proteins also are directly or indirectly involved in function or assembly of this cluster.

The lumen-exposed AB loop in the D2 protein, and particularly Glu69 in this loop, is important for proper functioning and stability of the water-splitting system (*9*, *13*, *14*). Several site-directed mutations have been introduced at the Glu69 position of D2, and the E69Q and E69V mutants have been characterized (*9*, *14*). The E69Q mutant is not able to grow photoautotrophically but evolves oxygen upon illumination. However, the rate decreases rapidly upon illumination, most likely due to photoinactivation. Addition of Mn^{2+} ions stabilizes the rate of oxygen evolution in this mutant. The E69V mutant degrades its core polypeptides in PS II very rapidly (*14*), suggestive of improper assembly in this strain.

Upon selection for photoautotrophic growth, one can isolate colonies of the E69Q mutant that still retain this mutation but are able to grow reasonably well without a fixed carbon source. They appear at a frequency of about 10^{-7}, in line with what would be expected for secondary mutations. The mapping of the secondary mutation and the characterization of the protein at this locus are the focus of this study.

MATERIALS AND METHODS

Growth Conditions. Synechocystis sp. PCC 6803 cells were grown at 28 °C at a light intensity of 40 μmol of photons m^{-2} s^{-1} in BG11 medium (*15*) supplemented with 5 mM glucose. Liquid cultures were grown while being shaken at 120 rpm. Solid medium was supplemented with 1.5% (w/v) agar, 0.3% (w/v) sodium thiosulfate, and 10 mM TES/NaOH buffer, pH 8.2. The PS II inhibitor atrazine (20 μM) was added to solid medium to maintain obligate photoheterotrophic mutants with defects in PS II and to avoid inadvertent selection for photoautotrophic (pseudo)revertants.

Growth rates upon Ca^{2+} or Cl^- depletion were determined upon photomixotrophic growth of *Synechocystis* sp. PCC 6803 at 28 °C in regular BG11 medium supplemented with 5 mM glucose (control) or in BG11 medium lacking Ca^{2+} or Cl^- but containing 5 mM glucose. In Ca^{2+}-less BG11 medium, $CaCl_2$ (0.24 mM) was replaced by 0.48 mM NaCl.

† This work is supported by a grant from the National Science Foundation (MCB-9728400) to W.F.J.V.

* Corresponding author. Phone: (480) 965-3698. Fax: (480) 965-6899. E-mail: galya@imap3.asu.edu.

[1] Abbreviations: Chl, chlorophyll; DCMU, 3-(3,4-dichlorophenyl)-1,1-dimethylurea; DMBQ, 2,5-dimethyl-*p*-benzoquinone; EDTA, disodium ethylenediaminetetraacetate; HEPES, *N*-(2-hydroxyethyl)-piperazine-*N*′-2-ethanesulfonic acid; TES, *N*-tris(hydroxymethyl)methyl-2-aminoethanesulfonic acid; PS II, photosystem II.

10.1021/bi0026526 CCC: $20.00
Published on Web 07/12/2001

The final concentration of Ca^{2+} in Ca^{2+}-less BG11 was less than 1.25 μM, the level of Ca^{2+} found in the doubly distilled water that was used for these studies. In Cl^--less BG11 medium, $CaCl_2$ (0.24 mM) and $MnCl_2$ (9.15 μM) were replaced by equal concentrations of $CaSO_4$ and $MnSO_4$. Moreover, $NaNO_3$ (17.6 mM) was substituted by the same concentration of KNO_3, because commercially available KNO_3 generally contains a lower level of contaminating Cl^-. The final concentration of Cl^- was 48 μM; this is 10 times less than that in regular BG11 medium. The light intensity was maintained at 40 μmol of photons m^{-2} s^{-1}. If growth rates were to be determined under photoautotrophic conditions, the cultures were grown as described above, except that glucose was omitted from the growth medium.

To determine the sensitivity of *Synechocystis* sp. PCC 6803 to high temperature, cells were grown at 39 °C; the light intensity and medium composition were as described above.

The optical density of cell cultures was determined at 730 nm using a Shimadzu UV-160 spectrophotometer.

Chromosomal DNA Isolation and Fractionation. Chromosomal DNA was isolated as described in ref *16*. After digestion of the chromosomal DNA with restriction endonucleases (*Bsa*BI, *Eco*RV, *Kpn*I, *Nhe*I, *Pst*I, *Sca*I, or *Xba*I), size fractionation was performed on a 0.5% (w/v) agarose gel in TBE buffer (0.089 M Tris base, 0.089 M boric acid, yielding a final pH of 8.0, and 2 mM EDTA). The gel was soaked in doubly distilled water for 30 min with gentle agitation and briefly stained with ethidium bromide. Every lane of the gel was sliced into 14 pieces, each representing a specific size range between 0.8 and 35 kbp. For DNA elution from the gel, agarose slices were incubated at −80 °C overnight, thawed at 37 °C for 3 h, and spun in a microcentrifuge at 14 000 rpm for 15 min. The supernatant was frozen at −80 °C overnight to reduce possible bacterial contamination and used for transformation of the E69Q strain of *Synechocystis* sp. PCC 6803 without further purification.

Complementation of the E69Q Mutant. E69Q mutant cells were harvested in mid-log phase (OD_{730} about 0.5) and concentrated to $OD_{730} = 20$, and 20 μL of this culture was incubated with 200 μL of each DNA sample for 6 h at room temperature and spotted on BG11 agar plates. Colonies of photoautotrophic transformants were visible after 10−12 days of incubation at 28 °C in the light at 40 μmol of photons m^{-2} s^{-1}.

Oxygen Evolution Assay. The steady-state rate of oxygen evolution in intact cells was determined using a Clark-type electrode at a chlorophyll concentration of 5 μg mL^{-1}. Measurements were performed in BG11 medium buffered with 25 mM HEPES/NaOH, pH 7.0, with 0.1 mM 2,5-dimethyl-*p*-benzoquinone (DMBQ) and 0.5 mM $K_3[Fe(CN)_6]$ as electron acceptors. The light from a 300 W Osram halogen lamp was filtered through a Schott OG-570 filter before reaching the sample and was saturating for maximal electron-transfer rates (1500 μmol of photons m^{-2} s^{-1}).

The time needed for the oxygen evolution rate to be reduced to 50% of the original rate was determined from oxygen evolution curves measured as described above but in the presence of 1 mM DMBQ and 5 mM $K_3[Fe(CN)_6]$ and at an incident intensity of white light of 5000 μmol of photons m^{-2} s^{-1}. This corresponds to a light intensity of 2200 μmol of photons m^{-2} s^{-1} when passed through a Schott OG-570 filter.

Light-induced loss of oxygen-evolving activity in the absence of de novo protein biosynthesis was determined using liquid cultures of *Synechocystis* sp. PCC 6803 ($OD_{730} = 0.2$) grown in normal or Ca^{2+}-depleted BG11 medium supplemented with 5 mM glucose. Cultures were incubated with 200 μg mL^{-1} lincomycin in the light (50 μmol of photons m^{-2} s^{-1}) on a rotary shaker, and the oxygen evolution rate of culture samples was measured as a function of incubation time. To determine oxygen evolution rates, 0.1 mM DMBQ and 0.5 mM $K_3[Fe(CN)_6]$ were present as electron acceptors in the oxygen electrode vessel.

Dark Decay of Oxygen Evolution Activity and Photoactivation. The oxygen evolution capacity of intact cells incubated in darkness at room temperature was measured as described (*17*).

Photoactivation was performed on hydroxylamine-treated cells essentially as described (*17*). Cells of wild-type and E69Q strains and of corresponding strains lacking *slr0286* were concentrated to 200 μg of Chl mL^{-1} in buffer containing 10 mM HEPES/NaOH, pH 7.2, 30 mM NaCl, 1 mM $CaCl_2$, and 50 μM $MnCl_2$ and were subsequently incubated with 2 mM hydroxylamine in total darkness for 10 min with agitation. Cells were then pelleted at 6000*g* at room temperature for 5 min and resuspended to 10-fold the original suspension volume in the same buffer. The pelleting and resuspension steps were repeated five times to wash out hydroxylamine. After the last wash, cells were resuspended to 200 μg of Chl mL^{-1}. For photoactivation hydroxylamine-extracted cells were placed on a rotary shaker under continuous illumination (15 μmol of photons m^{-2} s^{-1}). Fifty microliter aliquots were withdrawn at set time intervals for determination of the light-saturated rate of oxygen evolution in the presence of DMBQ as described above. The activity of oxygen evolution of hydroxylamine-treated cells did not increase further after 45 min illumination and at that time was about 85% of the activity of cells without hydroxylamine treatment.

Fluorescence Yield Decay Kinetics. The kinetics of decay of the chlorophyll fluorescence yield of intact cells were obtained using a Walz fluorometer (PAM 101, 102) after actinic illumination of intact cells in the presence of 40 μM 3-(3,4-dichlorophenyl)-1,1-dimethylurea (DCMU) essentially as described (*18*).

77 K Fluorescence Spectra. Low-temperature fluorescence emission spectra were recorded upon excitation of cell suspensions (chlorophyll concentration 1 μg mL^{-1}) by monochromatic light at 435 nm using a FluoroMax spectrofluorometer (Spex Industries, Inc.). The relative amount of intact PS II reaction center complexes compared to that of PS I centers was estimated from the ratio of the fluorescence emission amplitude at 695 nm over that at 725 nm. The fluorescence intensities were corrected for a small amount of background signal detected by the photomultiplier at 650 and 800 nm.

RNA Isolation and RT-PCR. Total RNA isolation from wild-type cells of *Synechocystis* sp. PCC 6803 was performed as described (*19*, *20*). The reverse transcription reaction step was conducted at 47 °C for 1 h. The polymerase chain reaction step consisted of 30 cycles, each of which included incubation at 94 °C for 30 s, 62 °C for 30 s, and 72 °C for 45 s. For quantitative analysis, 10 μL aliquots were with-

Table 1: Sequence of Primers Used for RT-PCR in This Study and Their Positions in the Genome of *Synechocystis* sp. PCC 6803[a]

Primer	Sequence	Position
5′ *slr0286*	5′GCT AAT ACA GCA AGT CAG CCA ATC3′	2125217-2125240
3′ *slr0286*	5′GAA TAG CAT TGT AGC TGG GCC GGC3′	2125601-2125578
5′ *psbDI*	5′CTT CGG CCA TTC CCT CCT GTT CCT3′	1349647-1349624
3′ *psbDI*	5′GTG TTT TCC ACC GTG GCA CCG TGG3′	1349237-1349260
5′ *slr0285*	5′TCT ATA TGA GCA GTG TGA CCG ATC3′	2124375-2124398
3′ *slr0285*	5′GGC TGT ATA ACT ATC CTG TCA ACT3′	2124780-2124757

[a] Numbering according to CyanoBase.

drawn from the RT-PCR reaction tubes after a certain number of PCR cycles. The amount of PCR product was determined by ethidium bromide staining after separation on a 1.2% (w/v) agarose gel. Standard size markers were from Gibco BRL. The transcription level of *slr0286* compared to that of *psbDI* was determined by RT-PCR with the primers described in Table 1. The priming efficiency of primers used for RT-PCR of these two genes was compared by PCR using the conditions described above and using equal amounts of genomic DNA from wild-type cells as template. To determine if the transcript level of *slr0285* was affected by the deletion of *slr0286*, RT-PCR was conducted under the conditions described above using total RNA obtained from both E69Q and Δ*slr0286*/E69Q cells and primers described in Table 1. All reagents were from Gibco BRL.

RESULTS

Isolation and Characterization of Pseudorevertants of the psbDI Mutant E69Q. The *Synechocystis* sp. PCC 6803 *psbDI* mutant E69Q is not able to grow photoautotrophically due to an apparent instability of water-splitting activity (*9*). This mutant lacks *psbDII* (the second gene coding for the D2 protein of PS II). Upon selection for photoautotrophic growth spontaneous photoautotrophic mutants were isolated. For one of them, named MQ2, the *psbDIC* gene cluster was amplified by PCR and sequenced. This strain retained the E69Q mutation in the *psbDI* gene and had no additional mutations in this gene cluster (data not shown). Indeed, PCR-amplified *psbDIC* from the MQ2 pseudorevertant did not complement E69Q to photoautotrophic growth whereas total genomic DNA isolated from the MQ2 pseudorevertant transformed the E69Q mutant with high frequency. Therefore, the site of the secondary mutation that led to the photoautotrophic phenotype was located outside of the *psbDIC* gene cluster.

Mapping of the Secondary Mutation Site. Initially, genes or gene clusters coding for PS II proteins that might have domains close to the manganese cluster (including *psbA*, *psbB*, *psbEFLJ*, *psbO*, and *psbV*) together with their flanking regions were amplified by PCR from MQ2 genomic DNA and tested regarding their capability to complement the E69Q mutant to photoautotrophic growth. None of them complemented E69Q to photoautotrophic growth, indicating that the secondary mutation was located outside the genes encoding structural proteins that are likely to be close to the manganese cluster.

To determine the locus of the secondary mutation, complementation mapping based on analysis of the size of complementing restriction fragments (*21*) was applied, making use of the genomic restriction map of *Synechocystis* sp. PCC 6803 for these enzymes. Genomic DNA from the MQ2 pseudorevertant was digested with *Bsa*BI, *Eco*RV, *Kpn*I, *Nhe*I, *Pst*I, *Sca*I, or *Xba*I and size-separated on a 0.5% (w/v) agarose gel. Each lane containing DNA fragments between 0.8 and 35 kbp was cut into 14 slices. DNA was extracted from every fraction and used for E69Q transformation. Only one DNA size fraction in each of six restriction digestions (all except for *Xba*I) was able to functionally complement the E69Q mutant, thus indicating that these fractions contained the fragment with the secondary mutation locus (Table 2). However, complementation was not observed after transformation of E69Q with restriction fragments generated by *Xba*I (Table 2). This could indicate either that the secondary mutation locus is very close to the restriction site for this enzyme, leaving insufficient flanking region for effective transfer of the secondary mutation during the homologous recombination, or that the secondary mutation site is located in a fragment less than 0.8 kb or larger than 35 kb, which were excluded from the complementation test.

Table 2: Comparison between the Experimental MQ2 Restriction Fragment Sizes That Complemented the E69Q Mutant to Photoautotrophic Growth and the Theoretical Restriction Pattern of the Sole Region of the *Synechocystis* sp. PCC 6803 Genome That Fits These Criteria

enzyme	size range of DNA fragments in the complementing fraction, kb	position of DNA fragment with the secondary mutation (CyanoBase numbering)	actual size of the fragment, bp
*Bsa*BI	1.0−1.5	2 124 514−2 125 895	1382
*Eco*RV	3.0−4.0	2 122 475−2 125 543	3069
*Kpn*I	4.0−5.0	2 121 757−2 126 662	4906
*Nhe*I	2.0−2.5	2 124 567−2 127 054	2488
*Pst*I	10.0−12.0	2 122 015−2 133 200	11186
*Sca*I	2.0−2.5	2 123 795−2 126 176	2382
*Xba*I	*a*	2 121 796−2 125 116	3321

[a] *Xba*I fragments did not complement E69Q to photoautotrophic growth. The position and the size of *Xba*I fragments were determined after the site of the pseudoreversion had been mapped, and it turned out that these fragments did not complement because one of the restriction sites for this enzyme (2 125 116) was very close to the secondary mutation site (2 125 090).

The size ranges of restriction fragments that were obtained from the functional complementation assay were compared with the size-sorted restriction map of the entire *Synechocystis* sp. PCC 6803 genome (*21*), and a single region with this specific restriction pattern was determined. The only genomic location that yields these sizes of restriction fragments for each employed endonuclease was the region from nucleotide

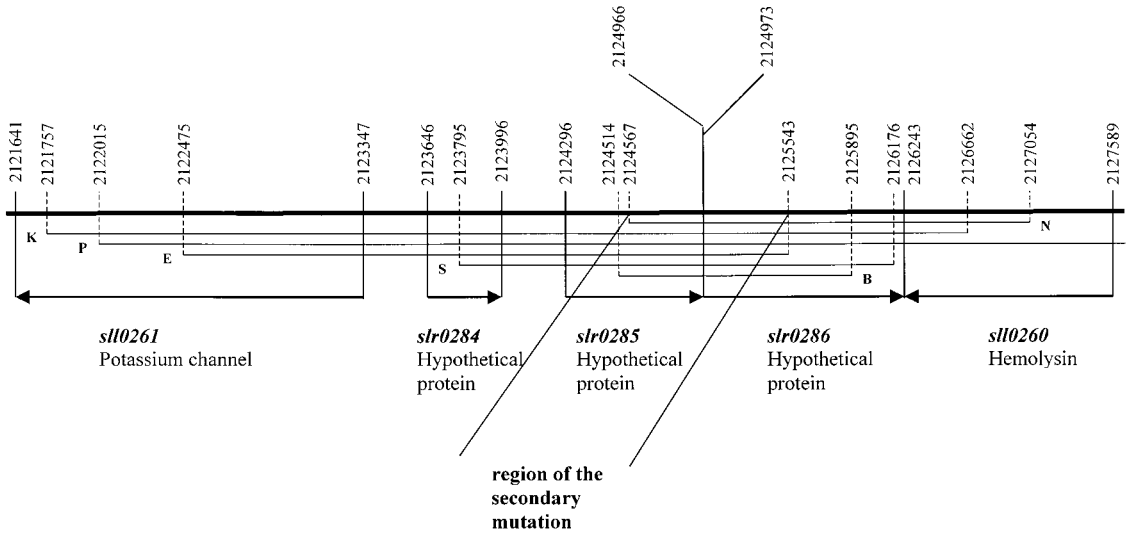

FIGURE 1: Location of the secondary mutation site in the genome of a photoautotrophic pseudorevertant of the E69Q (D2 protein) mutant of *Synechocystis* sp. PCC 6803. Restriction fragments that complement E69Q to photoautotrophic growth are shown by lines with the corresponding restriction enzymes indicated: *Bsa*BI (B), *Eco*RV (E), *Kpn*I (K), *Nhe*I (N), *Pst*I (P), and *Sca*I (S).

2 124 567 (an *Nhe*I site) to 2 125 543 (an *Eco*RV site) (numbering according to CyanoBase), corresponding to a 977 base pair fragment covering part of the open reading frames *slr0285* and *slr0286* (Figure 1).

To verify these findings, the genome region containing *slr0285* and *slr0286* plus 400 bp flanking regions on both sides was amplified by PCR from the MQ2 pseudorevertant and from the wild type and cloned into pUC18 yielding plasmids pMQ2 and pWT, respectively. Both plasmids were used to transform the E69Q mutant. Only pMQ2 but not pWT complemented E69Q to photoautotrophic growth, thus confirming the accuracy of the mapping.

The Genome Region Containing the Site of Pseudoreversion. The *Nhe*I/*Eco*RV fragment carrying the secondary mutation includes two partial open reading frames, *slr0285* and *slr0286*, that overlap by 8 bp and are likely to be cotranscribed (Figure 1). Surprisingly, the translated *slr0285* and *slr0286* open reading frames have no significant similarity to hypothetical or known proteins in the database and also have no homologues in the sequenced regions of other cyanobacteria such as *Anabaena* sp. PCC 7120, *Nostoc punctiforme*, and *Prochlorococcus marinus*.

To further narrow down the site of the secondary mutation, the pMQ2 plasmid carrying *slr0285* and *slr0286* and 400 bp flanking regions at each side was subcloned, giving two plasmid constructs: pΔslr0285 [carrying all of *slr0286* as well as *slr0285* from codon 156 onward (a *Hin*cII restriction site)] and pΔslr0285/0286 [carrying *slr0286* from codon 194 (an *Eco*RV restriction site) onward and lacking all of *slr0285*]. These plasmids were used to transform the E69Q mutant. Only pΔslr0285 was capable to transform E69Q to photoautotrophic growth whereas pΔslr0285/0286 was not. Therefore, the secondary mutation was located in a 782 base pair *Hin*cII/*Eco*RV fragment covering the 3′ end of *slr0285* and the 5′ end of *slr0286*. Sequencing of this fragment from MQ2 and wild type revealed a R42M mutation in Slr0286 in MQ2 due to a G to T change in nucleotide 2 125 090. The *slr0285* open reading frame was not altered.

Another photoautotrophic pseudorevertant of the E69Q mutant was mapped to the same region as MQ2. The PCR product corresponding to *slr0285* and *slr0286* (including 400 bp flanking regions at each side) from this pseudorevertant complemented E69Q to photoautotrophic growth. Sequencing revealed a R394H mutation in Slr0286 in this pseudorevertant.

Both mutations in *slr0286* complemented only the E69Q mutant but not other photoheterotrophic *psbDI* mutants of *Synechocystis* sp. PCC 6803 with mutations introduced at the donor (T192H) or acceptor [D2R8 (*16*)] side of PS II.

Deletion of slr0286. To check whether the R42M and R394H mutations lead to functional inactivation of Slr0286, a plasmid was constructed (pΔslr0286) in which the *Swa*I/*Cla*I fragment of *slr0286* from MQ2 (codons 148−311 of this open reading frame) was replaced by the *Hin*dII/*Sma*I fragment of the chloramphenicol (Cm) resistance cassette from pACYC184 (*22*). This construct was used for transformation of both the wild type and E69Q mutant of *Synechocystis* sp. PCC 6803, selecting for resistance to chloramphenicol. The complete segregation of the introduced deletion was demonstrated by PCR using the same primers as for amplification of *slr0285*/*slr0286* (including 400 bp flanking regions on each side). As indicated in Figure 2, the 2.7 kbp band present in the control is absent in the deletion mutant.

Physiological Consequences of Deleting Slr0286. (1) Growth Rate and Oxygen Evolution Activity. Inactivation of *slr0286* in wild type did not change the doubling time upon photoautotrophic growth or the oxygen evolution activity of the strain. The resulting Δ*slr0286*/E69Q mutant was not photoautotrophic, indicating that the two mutations in *slr0286* restoring photoautotrophic growth in E69Q did not do so by loss of Slr0286. One of the features of E69Q was instability of oxygen-evolving activity, particularly at high light intensity (*9*). For this reason, the stability of oxygen evolution upon illumination at high light intensity was monitored. This stability remained unaffected by the deletion of *slr0286* in both wild type and E69Q (Table 3). However, the stability of oxygen evolution of the MQ2 pseudorevertant was similar to that of wild type, suggesting that the instability of oxygen evolution of E69Q at high light intensity is the

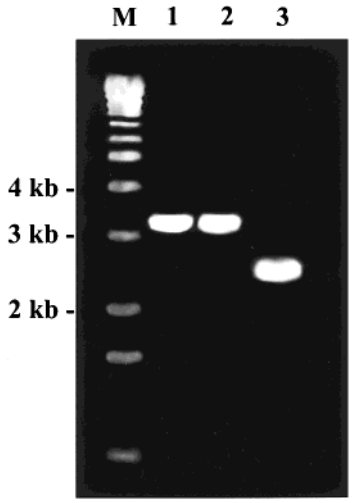

FIGURE 2: Segregation of the *slr0286* deletion in the E69Q mutant and wild type. PCR products of the locus containing *slr0285*, *slr0286*, and a 400 bp flanking region on each side were obtained using DNA of the Δ*slr0286*/WT (1), Δ*slr0286*/E69Q (2), and wild-type (3) strains. A marker lane (M) has been indicated on the left, and sizes have been indicated.

Table 3: Stability of Oxygen Evolution in Intact Cells of Wild Type (WT), the E69Q Mutant, the MQ2 Pseudorevertant, and the Δ*slr0286* Deletion Mutants in a Wild Type and E69Q Background of *Synechocystis* sp. PCC 6803 upon Strong Illumination (2200 μmol of photons m^{-2} s^{-1})[a]

	strain				
	WT	E69Q	MQ2	Δ*slr0286*/WT	Δ*slr0286*/E69Q
$t_{1/2}$, min	9.4 ± 1.0	5.6 ± 0.5	9.6 ± 0.9	9.4 ± 0.9	5.8 ± 0.7

[a] Oxygen evolution was measured at a chlorophyll concentration of 15 μg mL^{-1}. See Materials and Methods for further details. Values shown are the mean and standard deviations from three independent experiments.

reason for its obligate photoheterotrophic phenotype. The secondary mutation in Slr0286 reverses this phenotype, suggesting an effect of Slr0286 on the properties of the oxygen-evolving complex.

The increased stability of oxygen evolution and the restoration of photoautotrophic growth in the pseudorevertant could be due either to increased stabilization of assembled PS II complexes or to enhanced repair of damaged PS II centers. To distinguish between these two possibilities, the oxygen evolution capacity was followed in cell cultures that were incubated in the light in the presence of 200 μg mL^{-1} lincomycin. As shown earlier (*23*), even at half the lincomycin concentration that was used in our experiments protein biosynthesis in *Synechocystis* sp. PCC 6803 is blocked quantitatively. As shown in Figure 3, oxygen-evolving activity in the presence of lincomycin decreased at a similar rate in wild type and the MQ2 pseudorevertant, and this rate was higher for E69Q. The deletion of *slr0286* in either wild type or E69Q did not influence this decline in the oxygen evolution capacity. Therefore, the restoration of photoautotrophic capacity in the pseudorevertant appears to be due primarily to an increased functional stability of assembled PS II complexes rather than to a faster de novo resynthesis of damaged PS II components.

As the oxygen-evolving complex is rather heat labile, we investigated whether deletion of *slr0286* caused an alteration

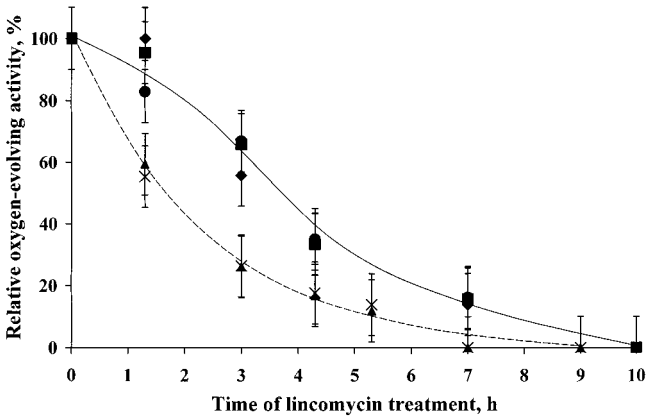

FIGURE 3: Loss of oxygen-evolving activity of wild type (◆), MQ2 pseudorevertant (●), and E69Q (▲) cells retaining *slr0286* and of wild type (■) and E69Q (×) lacking *slr0286* when grown in the light in the absence of de novo protein biosynthesis. Solid line: wild type (with and without *slr0286*) and pseudorevertant. Broken line: E69Q mutant regardless of the presence of *slr0286*. Cell cultures were grown in BG11 medium supplemented with 5 mM glucose at 50 μmol of photons m^{-2} s^{-1} in the presence of 200 μg mL^{-1} lincomycin. The oxygen evolution rate has been represented relative to values obtained for each strain before lincomycin treatment. Values represent the mean and standard deviation from three independent experiments.

in the heat tolerance of cells. Cultures of wild type and E69Q and the corresponding Δ*slr0286* mutants were grown photomixotrophically at 39 °C at 40 μmol of photons m^{-2} s^{-1}. The elevated growth temperature led to a 20−25% increase in the doubling time of all strains, but the *slr0286* deletion had no significant effect on either the photoautotrophic or photomixotrophic growth rate of wild type or the photomixotrophic growth rate of the E69Q mutant of *Synechocystis* sp. PCC 6803 (data not shown). However, the oxygen evolution activity of cells grown at high temperature was reduced after the deletion of *slr0286*. This effect was especially notable in the Δ*slr0286*/E69Q mutant in that it quickly lost all oxygen-evolving activity upon exposure to 39 °C (Figure 4). In the case of wild type, a modest decline in oxygen-evolving activity was observed for cells grown photomixotrophically and photoautotrophically, indicative of a gradual decline in oxygen-evolving activity in the absence of Slr0286. This phenotype in E69Q and to a lesser extent in the wild type suggests a role of Slr0286 in maintaining the oxygen-evolving activity of PS II. To further investigate the role of Slr0286 in this process, we examined the requirement of the strains studied here for Ca^{2+} and Cl^- (two ions needed for oxygen-evolving activity).

(2) Ca^{2+} and Cl^- Requirement of Cell Cultures upon slr0286 Deletion. Upon subculturing BG11-grown wild type and E69Q strains in BG11 medium from which Ca^{2+} had been omitted, in the strains lacking Slr0286 a more rapid decrease in oxygen evolution was observed than in strains retaining this protein (Figure 5). This effect was particularly apparent in E69Q, where in the second subculture no oxygen evolution could be observed if Slr0286 was absent. This suggests that the Ca^{2+} affinity of the oxygen-evolving complex is much decreased upon deletion of *slr0286*. However, the argument could be made that Slr0286 mutations might affect the efficiency of PS II repair and that the absence of Ca^{2+} merely enhanced PS II damage. To test this, the oxygen-evolving activity of *Synechocystis* sp. PCC 6803

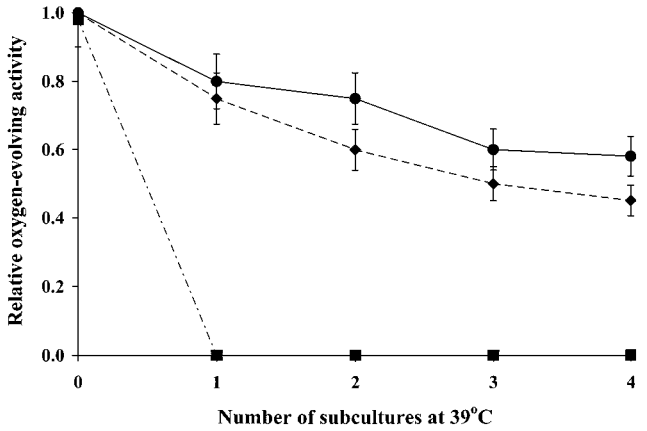

FIGURE 4: Oxygen-evolving activity of photomixotrophically (●) and photoautotrophically (◆) grown wild type and photomixotrophically grown E69Q (■) cells lacking *slr0286* relative to the same strains retaining *slr0286*. This activity has been plotted as a function of the number of subcultures that were propagated at 39 °C. Cells were subcultured by dilution to $OD_{730} = 0.03$ when the culture reached mid-exponential phase ($OD_{730} = 0.4-0.6$). Oxygen-evolving activities of the original (subculture number "0") cell cultures grown under photomixotrophic conditions (see Materials and Methods) were 241 ± 22 (wild type), 234 ± 21 (Δ*slr0286*/WT), 123 ± 22 (E69Q), and 113 ± 21 (Δ*slr0286*/E69Q) μmol of O_2 (mg of Chl)$^{-1}$ h^{-1}. After four subcultures, oxygen evolution activities of these strains were 204 ± 19, 126 ± 17, 47 ± 6, and 0 μmol of O_2 (mg of Chl)$^{-1}$ h^{-1}, respectively. Values represent the mean and standard deviation from five independent experiments.

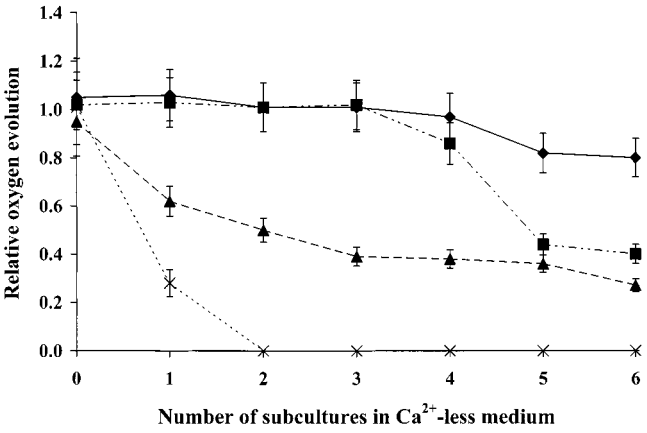

FIGURE 5: Oxygen evolution of wild type (◆) and E69Q (▲) cells retaining *slr0286* and of wild type (■) and E69Q (×) lacking *slr0286* upon subculturing in BG11 medium in which Ca^{2+} has been replaced by Na^+. The oxygen evolution rate has been represented relative to the oxygen-evolving activity of cultures subcultured in normal (Ca^{2+}-containing) BG11 medium. To both media 5 mM glucose had been added. Upon subculturing, cells in mid-exponential phase ($OD_{730} = 0.4-0.6$) were diluted to $OD_{730} = 0.03$. Values represent the mean and standard deviation from five independent experiments. For the oxygen-evolving activity of the original cell cultures grown under normal conditions (subculture 0 or subcultures in the presence of Ca^{2+}), see the legend to Figure 4.

cultures grown in Ca^{2+}-depleted medium in the presence of 200 μg mL^{-1} lincomycin was followed as a function of time. As shown in Figure 6, the activity decreased similarly in the wild type (regardless of the presence of Slr0286) and the pseudorevertant, and again a more rapid inactivation of oxygen evolution was seen in E69Q, regardless of the presence of Slr0286. Therefore, the effect of Slr0286 on apparent Ca affinity appears to be a direct one rather than one mediated through PS II repair.

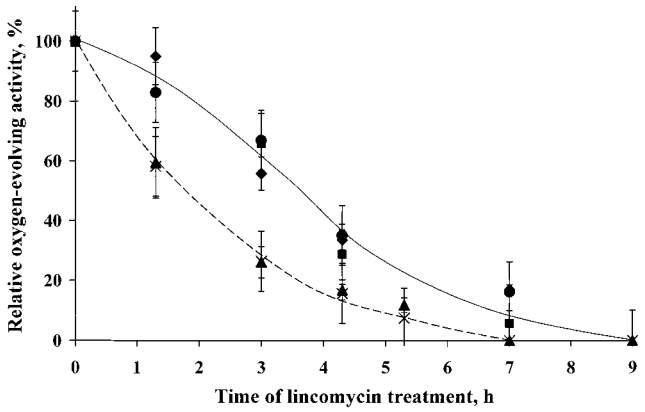

FIGURE 6: Oxygen-evolving activity of cells from wild type (◆), MQ2 pseudorevertant (●), and E69Q (▲) and of wild type (■) and E69Q (×) lacking *slr0286* grown in Ca^{2+}-depleted BG11 medium in the presence of 200 μg mL^{-1} lincomycin added at time 0. Cells were started from the culture grown in normal BG11 medium and diluted 20-fold in BG11 medium without Ca^{2+} to $OD_{730} = 0.02$. Cells were grown at 40 μmol of photons m^{-2} s^{-1} in BG 11 medium lacking Ca^{2+} to $OD_{730} = 0.5-0.6$. Values represent the mean and standard deviation from three independent experiments.

The *slr0286* deletion had no significant effect on the oxygen-evolving activity and growth rate of the wild type and E69Q mutant upon Cl^- depletion (data not shown).

(3) Other Donor Side Effects of the slr0286 Deletion. As the Ca^{2+} affinity of the oxygen-evolving complex apparently has been affected by the *slr0286* deletion, other properties of the donor side were investigated. As in mutants lacking cytochrome c_{550} the oxygen-evolving activity of PS II is labile in darkness (*24*), the stability of oxygen-evolving activity was assayed when cells with and without Slr0286 were incubated in darkness for 1 h. The oxygen-evolving activity of wild-type and E69Q cells decreased to about 80% and 70% of the original activity, respectively, regardless of the presence of Slr0286. Therefore, there was no evidence of a Slr0286 effect in this respect.

The second item to investigate was the kinetics of charge recombination between Q_A^- and the donor side of PS II. These kinetics are sensitive to the redox midpoint potential of donor side components such as the S_2/S_1 couple of the oxygen-evolving apparatus. The charge recombination kinetics were followed by monitoring the decay in the variable fluorescence yield using a PS I-less strain of *Synechocystis* sp. PCC 6803 (*25*). The charge recombination kinetics monitored as chlorophyll fluorescence yield decay (reflecting Q_A^- reoxidation) in the presence of 40 μM DCMU had a half-time of 250 ms in the PS I-less strain regardless of the presence of *slr0286* (data not shown).

The third property of the oxygen-evolving complex that was investigated was the kinetics of photoactivation of the water-splitting apparatus in *Synechocystis* sp. PCC 6803 cells after treatment with 2 mM hydroxylamine for 10 min. Hydroxylamine was washed out by five cycles of centrifugation and resuspension, and restoration of an active oxygen-evolving system upon illumination at 15 μmol of photons m^{-2} s^{-1} was followed as a function of time. In the Δ*slr0286* strains photoactivation kinetics were retarded slightly (Figure 7).

(4) Accumulation of PS II Complexes. To determine whether the impairment of oxygen evolution activity upon heat treatment or Ca^{2+} depletion in the Δ*slr0286* strains was

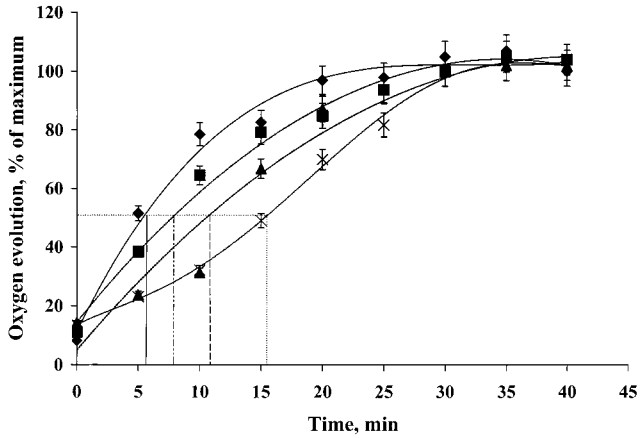

FIGURE 7: Photoactivation of wild type (◆) and E69Q mutant (▲) cells of *Synechocystis* sp. PCC 6803 and of wild type (■) and E69Q (×) upon *slr0286* deletion. The cells were treated with 2 mM hydroxylamine in darkness for 10 min, hydroxylamine was washed out, and cells were transferred to light (intensity: 15 μmol of photons m^{-2} s^{-1}). Oxygen-evolving activity was followed as a function of time of illumination. The maximum oxygen-evolving activity of hydroxylamine-treated cells was measured after 45 min of illumination and was 199 ± 17 (wild type), 201 ± 15 (Δ*slr0286*/WT), 102 ± 16 (E69Q), and 97 ± 13 (Δ*slr0286*/E69Q) μmol of O_2 (mg of Chl)$^{-1}$ h^{-1}. Values represent the mean and standard deviation from five independent experiments.

due to a disappearance of PS II or to an inactivation of PS II centers, the ratio of 77 K fluorescence emission at 695 and 725 nm was determined in intact cells upon excitation at 435 nm. In the first approximation, this ratio reflects the ratio of assembled PS II reaction center complexes (regardless of the presence of an intact oxygen-evolving system) and PS I (*26*). As illustrated in Table 4, the ratio of the fluorescence emission intensity at 695 and 725 nm remained stable for all strains upon subculturing at 39 °C or in Ca^{2+}-depleted medium. In addition, the 77 K fluorescence emission spectra in the 650−800 nm range did not change significantly (not shown). This implies that the effects of *slr0286* deletion on oxygen evolution upon growth at 39 °C or in the absence of Ca^{2+} were not due to a loss of PS II but rather to an inactivation of the oxygen-evolving complex of PS II.

Transcript Level of slr0286. On the basis of the results obtained so far, Slr0286 may function in cells of *Synechocystis* sp. PCC 6803 either as a protein involved in PS II assembly (possibly via the stabilization of folding of the AB loop of the D2 protein in PS II) and/or as a protein stabilizing the oxygen-evolving activity of PS II and contributing to a high-affinity Ca^{2+} binding site. However, there is no report that this protein has ever been found as a constitutive component of the PS II complex. To determine what the potential abundance of Slr0286 is, we conducted RT-PCR experiments on total RNA. Accumulation of the *slr0286* RT-PCR product lagged by 5−10 cycles as compared to that of *psbDI* (Figure 8A), indicating a very much reduced abundance of *slr0286* relative to the rather highly expressed *psbD* genes. Control experiments showed that PCR on these templates did not yield a product when reverse transcriptase was omitted, thus indicating the absence of DNA in the samples. Moreover, using genomic DNA as template, the amount of PCR product with the *psbDI* versus the *slr0286* primers was comparable (Figure 8B), indicating that the priming efficiency of both sets of primers used for the RT-PCR was similar. Therefore, the amount of *slr0286* transcript is much lower than that of a stoichiometric PS II component, in line with the argument that Slr0286 is involved with stabilization or assembly of the oxygen-evolving complex but is not a stoichiometric part thereof.

As deletion of *slr0286* could potentially lead to a change in abundance of *slr0285* transcript as the two may be cotranscribed (Figure 1), we checked *slr0285* abundance by RT-PCR using total RNA obtained from E69Q and Δ*slr0286*/E69Q cells (primers used in this experiment are listed in Table 1). The results are shown in Figure 9. Deletion of *slr0286* did not lead to an altered amount of *slr0285* transcript, thus excluding significant effects of the *slr0286* deletion on *slr0285* expression.

DISCUSSION

The product of the *Synechocystis* sp. PCC 6803 *slr0286* unidentified open reading frame appears to be involved in PS II donor side activity by interacting with Glu69 of the D2 protein. Slr0286 is predicted to be a 50.2 kDa protein consisting of 426 amino acid residues (Figure 10). There are two hydrophobic regions that may constitute transmembrane spans (Figure 10). Therefore, Slr0286 most likely is a membrane-anchored protein.

As mutations in Arg42 and Arg394 were shown to functionally complement the Glu to Gln mutation at residue 69 of the D2 protein, which is on the lumenal side of the membrane, these two residues of Slr0286 are expected to be on the lumenal side of the thylakoid. This implies that the N-terminus of Slr0286 should be transported through the thylakoid. Indeed, the N-terminal part of the protein has

Table 4: Accumulation of PS II Reaction Centers in Cells of Wild Type (WT), the E69Q Mutant, the MQ2 Pseudorevertant, and the Δ*slr0286* Deletion Mutants in a Wild Type and E69Q Background of *Synechocystis* sp. PCC 6803 Grown under Ca^{2+} Depletion Conditions or at High Temperature (39 °C)[a]

	ratio of 77 K fluorescence emission at 695 and 725 nm							
	no. of subcultures in Ca^{2+}-less medium				no. of subcultures at high temp (39 °C)			
strain	0	2	4	6	0	2	4	6
WT	0.15 ± 0.01	0.15 ± 0.01	0.14 ± 0.01	0.15 ± 0.01	0.15 ± 0.01	0.15 ± 0.01	0.16 ± 0.01	0.13 ± 0.01
E69Q	0.16 ± 0.01	0.15 ± 0.03	0.14 ± 0.01	0.15 ± 0.01	0.16 ± 0.01	0.13 ± 0.01	0.14 ± 0.01	0.14 ± 0.01
MQ2	0.17 ± 0.01	0.17 ± 0.01	0.14 ± 0.01	0.16 ± 0.01	0.17 ± 0.01	0.16 ± 0.01	0.15 ± 0.01	0.15 ± 0.01
Δ*slr0286*/WT	0.15 ± 0.01	0.14 ± 0.01	0.15 ± 0.01	0.17 ± 0.01	0.15 ± 0.01	0.16 ± 0.01	0.15 ± 0.01	0.14 ± 0.01
Δ*slr0286*/E69Q	0.15 ± 0.01	0.16 ± 0.01	0.14 ± 0.01	0.16 ± 0.01	0.15 ± 0.01	0.16 ± 0.01	0.14 ± 0.01	0.13 ± 0.01

[a] The relative amount of PS II reaction center complexes compared to PS I centers was estimated as the ratio of 77 K fluorescence emission intensities at 695 and 725 nm upon 435 nm excitation. Note that this ratio does not indicate whether PS II reaction center complexes have an intact and functional oxygen-evolving complex. The values represent the mean and standard deviation from three independent experiments.

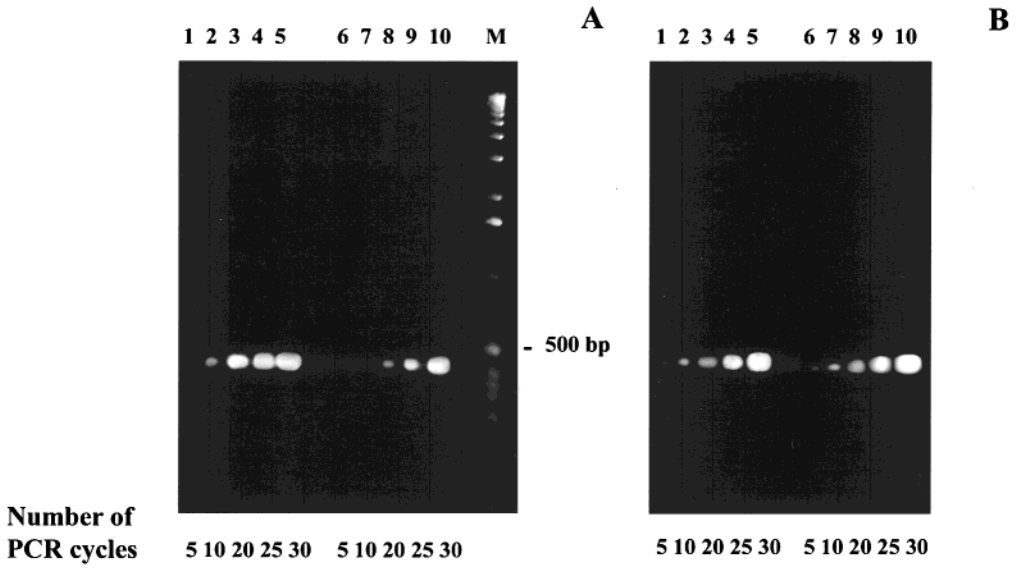

FIGURE 8: Accumulation of RT-PCR products corresponding to *psbDI* (lanes 1−5) and *slr0286* (lanes 6−10) transcripts using total RNA isolated from wild type *Synechocystis* sp. PCC 6803 as a template (A). Comparison of efficiency of primers used for RT-PCR of transcripts corresponding to *psbDI* (lanes 1−5) and *slr0286* (lanes 6−10) genes (B). The number of PCR cycles to which the samples have been exposed has been indicated. Molecular weight markers (M) are in the right lane in panel A.

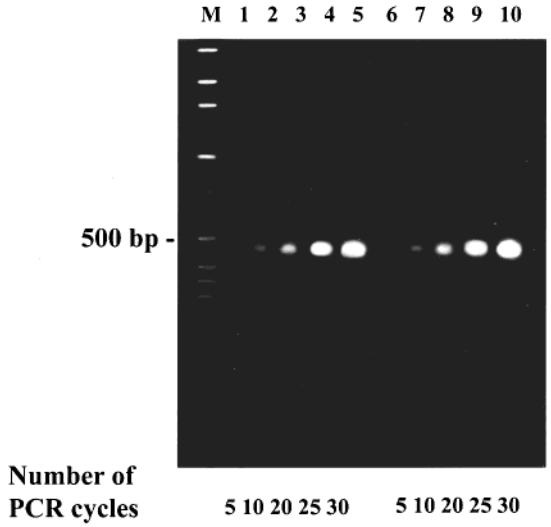

FIGURE 9: Accumulation of RT-PCR products corresponding to the *slr0285* transcript using total RNA isolated from E69Q (lanes 1−5) and from Δ*slr0286*/E69Q cells (lanes 6−10) of *Synechocystis* sp. PCC 6803 as a template. The number of PCR cycles to which the samples have been exposed has been indicated. Molecular weight markers (M) are in the lane to the left.

features consistent with a prokaryotic transit peptide (*27*−*29*): a positively charged N-terminal region ending at Arg25 and then a hydrophobic region. The transit peptide is likely to be cleaved off behind Ala35. Therefore, the N-terminus of Slr0286 is most likely to be targeted to and transported through the thylakoid membrane, and the mature protein is likely to be anchored in the membrane with most of the molecule being on the lumenal side of the membrane. This localization is in accordance with the apparent involvement of this protein in assembly of the oxygen-evolving complex of PS II.

The secondary mutations in Slr0286 caused restoration of photoautotrophic growth in the E69Q mutant but not in other photoheterotrophic mutants with changes in *psbDI* or other PS II genes. Moreover, none of the pseudorevertants generated for photoheterotrophic *psbDI* mutants other than for

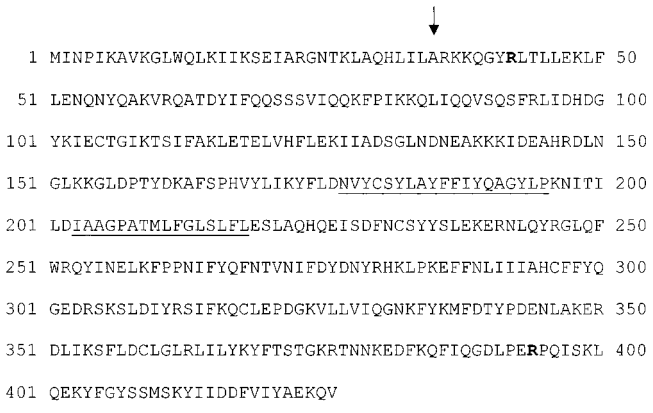

FIGURE 10: Primary structure of Slr0286 from *Synechocystis* sp. PCC 6803. Regions corresponding to the predicted transmembrane spans have been underlined, and Arg42 and Arg394 have been bolded. The putative cleavage site for lumenal targeting has been indicated by an arrow.

E69Q had their secondary mutation map to *slr0286* (for example, ref *16*). This suggests that Slr0286 interacts with the AB loop of the D2 protein but not with a large variety of other PS II domains.

Both second-site mutations in Slr0286 that reconstitute function in E69Q involve Arg residues being mutated to neutral or less positive ones. This suggests that the Arg residues may electrostatically interact with Glu69 of D2 and that removal of net charges on either of the constituents allows the interaction between Slr0286 and D2 to take place again.

The effect of the deletion of *slr0286* in wild type and E69Q was mild, suggesting that other proteins or nonenzymatic processes may functionally substitute, at least under laboratory conditions. The stability of a functional oxygen-evolving complex and the redox midpoint potential of the water-splitting complex remained unchanged upon deletion of *slr0286*, suggesting that a functionally normal water-splitting complex can be formed. However, the heat stability, Ca^{2+} affinity, and to some extent the photoactivation kinetics were

altered, suggesting a structural change in the complex. The photoactivation effect, opposite to that observed for Δ*psbO* (*17*, *30*), Δ*psbU*, and Δ*psbV* (*24*) mutants of *Synechocystis* sp. PCC 6803, could be caused by improper folding of proteins around the Mn or by an altered affinity of Mn.

The identification of Slr0286 as a protein involved in the assembly and/or stability of the oxygen-evolving complex of PS II brings up the question whether similar proteins can be found in other organisms. When searching for significant similarity of Slr0286 to other proteins, no matches were identified, not even when searching in the essentially completed genome sequences of other cyanobacteria (*Anabaena* sp. PCC 7120, *N. punctiforme*, and *P. marinus*). This may indicate that Slr0286 was functionally substituted by other proteins in chloroplasts and in other cyanobacteria. Glu69 is conserved in the D2 protein throughout evolution and is functionally important in *Chlamydomonas reinhardtii* (J.-D. Rochaix, personal communication).

In any case, using the pseudorevertant approach, we have identified an open reading frame coding for a protein that appears to be involved in functional assembly and folding of the water-splitting system.

REFERENCES

1. Green, B. R., and Durnford, D. G. (1996) *Annu. Rev. Plant Physiol. Plant Mol. Biol. 47*, 685−714.
2. Hankamer, B., Morris, E. P., and Barber, J. (1999) *Nat. Struct. Biol. 6*, 560−564.
3. Barber, J., and Kühlbrandt, W. (1999) *Curr. Opin. Struct. Biol. 9*, 469−475.
4. Debus, R. (1992) *Biochim. Biophys. Acta 1102*, 269−352.
5. Seidler, A. (1996) *Biochim. Biophys. Acta 1277*, 35−60.
6. Chu, H.-A., Nguyen, A. P., and Debus, R. J. (1995) *Biochemistry 34*, 5839−5858.
7. Chu, H.-A., Nguyen, A. P., and Debus, R. J. (1995) *Biochemistry 34*, 5859−5882.
8. Nixon, P. J., Trost, J. T., and Diner, B. A. (1992) *Biochemistry 31*, 10859−10871.
9. Vermaas, W., Charité, J., and Shen, G. (1990) *Biochemistry 29*, 5325−5332.
10. Knoepfle, N., Bricker, T. M., and Putnam-Evans, C. (1999) *Biochemistry 38*, 1582−1588.
11. Gleiter, H. M., Haag, E., Shen, J.-R., Eaton-Rye, J. J., Seeliger, A. G., Inoue, Y., Vermaas, W. F. J., and Renger, G. (1994) *Biochemistry 33*, 12063−12071.
12. Gleiter, H. M., Haag, E., Shen, J.-R., Eaton-Rye, J. J., Seeliger, A. G., Inoue, Y., Vermaas, W. F. J., and Renger, G. (1995) *Biochemistry 34*, 6847−6856.
13. Ermakova-Gerdes, S., Shestakov, S., and Vermaas, W. (1996) *Plant Mol. Biol. 30*, 243−254.
14. Yu, J., and Vermaas, W. F. J. (1993) *J. Biol. Chem. 268*, 7407−7413.
15. Rippka, R., Deruelles, J., Waterbury, J., Herdman, M., and Stanier, R. (1979) *J. Gen. Microbiol. 111*, 1−61.
16. Ermakova-Gerdes, S., and Vermaas, W. (1999) *J. Biol. Chem. 274*, 30540−30549.
17. Burnap, R., Qian, M., and Pierce, R. (1996) *Biochemistry 35*, 874−882.
18. Howitt, C. A., Udall, P. K., and Vermaas, W. F. J. (1999) *J. Bacteriol. 181*, 3994−4003.
19. Mohamed, A., and Jansson, C. (1989) *Plant Mol. Biol. 13*, 693−700.
20. Cooley, J. W., Howitt, C. A., and Vermaas, W. F. J. (2000) *J. Bacteriol. 182*, 714−722.
21. Vermaas, W. F. J. (1998) *Methods Enzymol. 297*, 293−310.
22. Chang, A. C. Y., and Cohen, S. W. (1978) *J. Bacteriol. 143*, 1141−1156.
23. Vermaas, W., Madsen, C., Yu, J. J., Visser, J., Metz, J., Nixon, P. J., and Diner, B. (1995) *Photosynth. Res. 45*, 99−104.
24. Shen, J.-R., Qian, M., Inoue, Y., and Burnap, R. L. (1998) *Biochemistry 37*, 1551−1558.
25. Shen, G., Boussiba, S., and Vermaas, W. F. J. (1993) *Plant Cell 5*, 1853−1863.
26. Haag, E., Eaton-Rye, J. J., Renger, G., and Vermaas, W. F. J. (1993) *Biochemistry 32*, 4444−4454.
27. Martoglio, B., and Dobberstein, B. (1998) *Trends Cell Biol. 8*, 410−415.
28. Fekkes, P., and Driessen, A. J. M. (1999) *Microbiol. Mol. Biol. Rev. 63*, 161−173.
29. Krimm, I., Gans, P., Hernandez, J.-F., Arlaud, G. J., and Lancelin, J.-M. (1999) *Eur. J. Biochem. 265*, 171−180.
30. Qian, M., Dao, L., Debus, R., and Burnap, R. (1999) *Biochemistry 38*, 6070−6081.

BI0026526